An Investigation of Steady-State Averaging for the Single-Inductor Dual-Output Buck Converter using Fourier Analysis

Ben Tsai, Olivier Trescases, Bruce Francis
University of Toronto, Department of Electrical and Computer Engineering
10 King's College Road, Toronto, ON, M5S 3G4, Canada

***Abstract*—The SIDO converter is appealing in low-power applications requiring two independent supply voltages. The use of a single inductor significantly reduces the cost and size of the converter, however the complexity of the controller is greatly increased due to the inherent coupling of the two output voltages in continuous conduction mode. The accuracy of the traditional averaging technique is examined for the SIDO converter and it is shown that using a Fourier-based analysis yields a much more accurate steady-state operating point, especially at light loads. The solution can be used to obtain accurate steady-state converter waveforms for a wide range of conditions without requiring lengthy transient simulations. The accurate operating point is also used to obtain the SIDO transfer functions for a synchronous 1 MHz SIDO buck converter. For a fixed duty cycle, the error in output voltage resulting from the standard averaging method can easily reach 25 % at light loads.**

I. Introduction

The steady-state analysis of switched-mode power supplies (SMPS) is usually carried out using the small-ripple approximation, in conjunction with inductor volt-second balance and capacitor charge balance [1]. This approach leads to simple closed-form expressions for the dc conversion ratio $M(D) = V_{out}/V_g$, which provides a reasonable accuracy for most basic topologies. In this paper a more accurate frequency-domain modeling technique is applied to the single-inductor, dual-output (SIDO) topology shown in Fig. 1(a). The ideal converter waveforms are shown in Fig. 1(b) for the converter operating in continuous conduction mode (CCM). The SIDO converter is attractive in low-power applications requiring two independent supply voltages V_1 and V_2, such as the I/O and core voltages for a microprocessor or for dynamic voltage scaling [2], [3]. The use of a single inductor significantly reduces the cost and size of the converter, while the complexity of the controller is greatly increased due to the inherent coupling of the two output voltages in continuous conduction mode [3]–[5]. A traditional steady-state model of the SIDO has been used for the design of linear controllers, leading to the following steady-state equations [6]:

$$\frac{V_1}{V_g} = \frac{D_A D_B R_1}{D_B^2 R_1 + (1-D_B)^2 \cdot R_2 + r_L}, \quad (1)$$

$$\frac{V_2}{V_g} = \frac{D_A (1-D_B) R_2}{D_B^2 R_1 + (1-D_B)^2 \cdot R_2 + r_L} \quad (2)$$

In these equations $0 < D_A < 1$ and $0 < D_B < 1$ are the two duty cycles, where the switches are assumed to be ideal, and R_1 and R_2 are the load resistances of the two outputs. The equations are only valid for the converter operating in continuous conduction mode (CCM), which is assumed for the remainder of this paper. The block diagram of the SIDO converter is shown in Fig. 2(a), where the circuit impedances are given by

$$Z_1(s) = R_1 \frac{r_1 C_1 s + 1}{(R_1 + r_1) C_1 s + 1}, \quad (3)$$

$$Z_2(s) = R_2 \frac{r_2 C_2 s + 1}{(R_2 + r_2) C_2 s + 1} \quad (4)$$

$$Y_L(s) = \frac{1}{Ls + r_L} \quad (5)$$

The multipliers in Fig. 2 result from the PWM signals $c_A(t)$ and $c_B(t)$. The convention is to approximate the average of the product $c(t) \cdot v(t)$ by the product of the averages. In many cases, such as simple buck and boost converters, this approximation is accurate. In more complex topologies such as the SIDO converter, the conventional averaging method leads to relatively poor accuracy, especially at light loads as we shall see. The purpose of this paper is to establish this point and to propose a correction in this case. The limitations of standard averaging methods under large ripple conditions have long been recognized [7]–[9].

II. Accurate Steady-State Operating Point

The following analysis is used to demonstrate that using frequency domain methods yields a much more accurate operating point compared to the traditional average method [1], especially in the case of the SIDO converter operating under light-load conditions. In steady-state, each electrical signal is periodic, of period $T_s = 1/f_s$, and therefore has a Fourier series of the form

$$v_1(t) = \sum_k v_1[k] w_k(t), \quad w_k(t) = \mathrm{e}^{j\omega_k t}, \quad \omega_k = \frac{2\pi}{T} k. \quad (6)$$

The sum is over all integers k, positive, negative, and zero, and ω_k is the k^{th} harmonic frequency. We use the notation $v_1[k]$ for the Fourier series coefficients of $v_1(t)$; notice that $v_1[-k]$ and $v_1[k]$ will be complex conjugates. Since the time

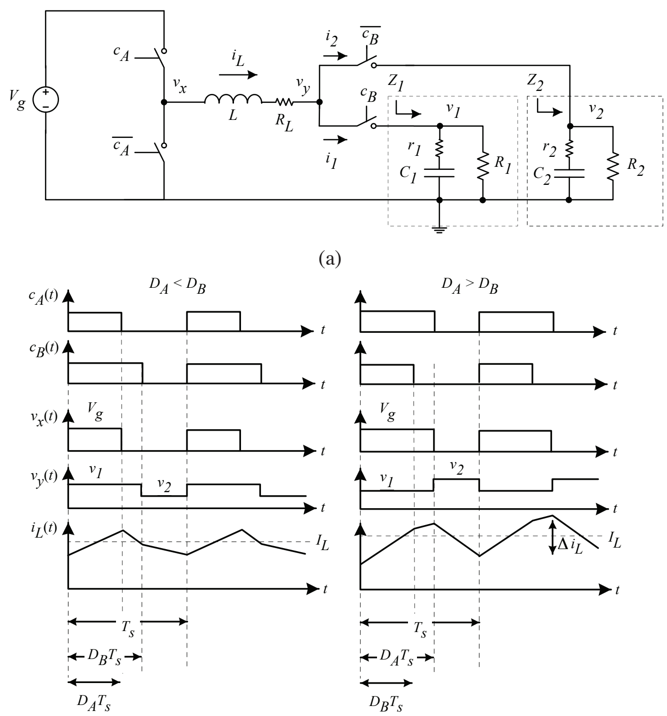

Fig. 1. Single-inductor dual-output buck converter.

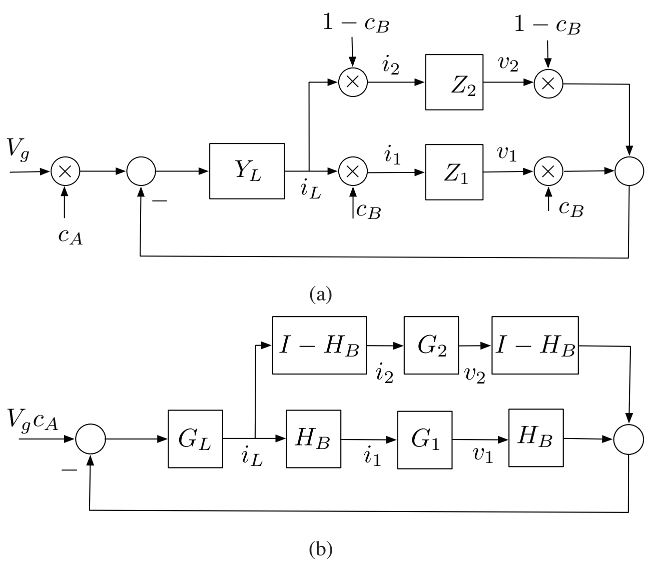

Fig. 2. Block diagram of the SIDO converter with (a) the multiplier blocks and (b) equivalent representation.

average over one period of $w_k(t)$ for $k \neq 0$ equals 0, the average of $v_1(t)$ equals $v_1[0]$, the zeroth Fourier coefficient. For the product of two signals, $y(t) = c_B(t)v_1(t)$, the Fourier coefficients of the three signals satisfy

$$y[k] = c_B[0] * v_1[k] = \sum_n c_B[k-n]v_1[n], \qquad (7)$$

where the star denotes discrete-time convolution. Thus the time average of $y(t)$ satisfies

$$y[0] = \sum_n c_B[-n]v_1[n], \qquad (8)$$

and not the product $c_B[0]v_1[0]$ as in standard practice.

The vectors of coefficients are infinite dimensional; for example

$$v_1 = \left[\begin{array}{c} \vdots \\ v_1[-2] \\ v_1[-1] \\ \hline v_1[0] \\ v_1[1] \\ \vdots \end{array}\right].$$

The horizontal line is just a place-marker; the vector has an infinite number of components going up from the line and going down from the line. These vectors are square summable. Then the equations are written for the vectors and the corresponding block diagram is shown in Fig. 2(b). The symbols G_L, H_B etc. represent matrices of infinite dimensions. For example G_L is the diagonal matrix,

$$G_L = \left[\begin{array}{cccc|cccc} & \vdots & \vdots & & \vdots & \vdots & \vdots & \\ \cdots & 0 & Y_L(j\omega_{-1}) & & 0 & 0 & 0 & \cdots \\ \hline \cdots & 0 & 0 & & Y_L(j\omega_0) & 0 & 0 & \cdots \\ \cdots & 0 & 0 & & 0 & Y_L(j\omega_1) & 0 & \cdots \\ & \vdots & \vdots & & \vdots & \vdots & \vdots & \end{array}\right]$$

while G_1 and G_2 are identical to G_L with Y_L replaced by Z_1 and Z_2 respectively. On the other hand, the matrix H_B comes from the convolution equation (8):

$$H_B = \left[\begin{array}{ccc|cccc} & \vdots & \vdots & \vdots & \vdots & \vdots & \\ \cdots & c[0] & c[-1] & c[-2] & c[-3] & c[-4] & \cdots \\ \cdots & c[1] & c[0] & c[-1] & c[-2] & c[-3] & \cdots \\ \hline \cdots & c[2] & c[1] & c[0] & c[-1] & c[-2] & \cdots \\ \cdots & c[3] & c[2] & c[1] & c[0] & c[-1] & \cdots \\ \cdots & c[4] & c[3] & c[2] & c[1] & c[0] & \cdots \\ & \vdots & \vdots & \vdots & \vdots & \vdots & \end{array}\right]$$

Such a matrix, constant along the diagonals, is a Toeplitz matrix. Of course, for computations, the vectors and matrices are contracted to being finite dimensional. From the block diagram in Fig. 2(b), the following equation is valid:

$$i_L = G_L[V_gc_A - H_BG_1H_Bi_L - (I-H_B)G_2(I-H_B)i_L]. \qquad (9)$$

Thus

$$i_L = [I + G_LH_BG_1H_B + G_L(I-H_B)G_2(I-H_B)]^{-1}G_LV_gc_A \qquad (10)$$

and the output voltages are given by

$$v_1 = G_1H_Bi_L \qquad (11)$$

$$v_2 = G_2(I-H_B)i_L. \qquad (12)$$

The convention $V_1\{N\}$ is used to denote the average value of V_1, where all Fourier coefficients up N have been used when solving (12). A MATLAB script was designed to determine $V_1\{N\}$ and $V_2\{N\}$ for different values of N, by solving (12) and taking the average over one cycle of T_s. Note that $V_1\{0\}$ and $V_2\{0\}$ give the same result as the standard averaging method of (2). The steady-state output voltages $V_1\{N\}$ and $V_2\{N\}$ are plotted versus D_B for N = 0 and N = 10 with D_A = 0.6 in Fig. 3(a).

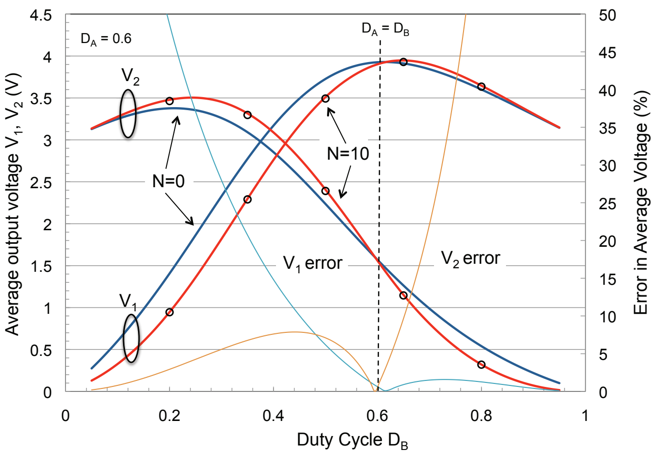

(a)

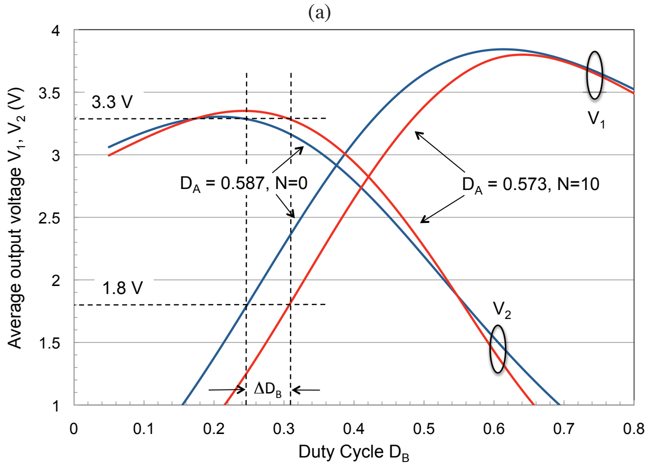

(b)

Fig. 3. (a) Steady-state output voltages V_1 and V_2 versus D_B using N=0 and N=10. The circles correspond to transient simulation results. (b) V_1 and V_2 versus D_B showing the operating points for V_1=1.8 V and V_2 = 3.3 V.

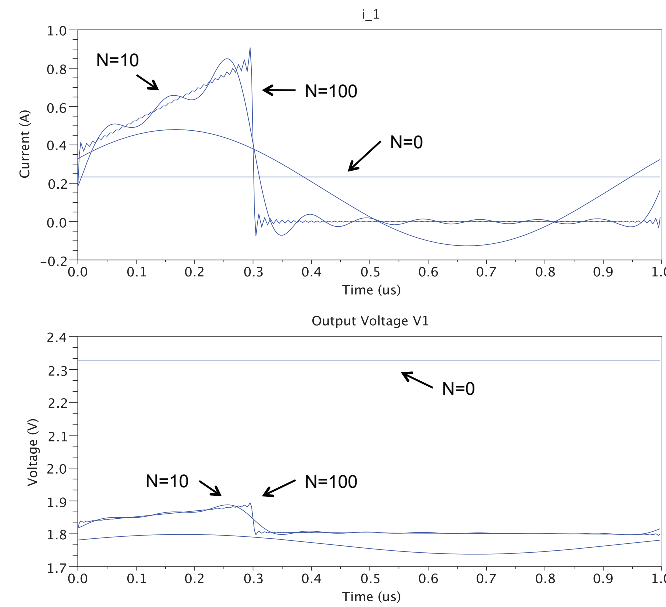

(a)

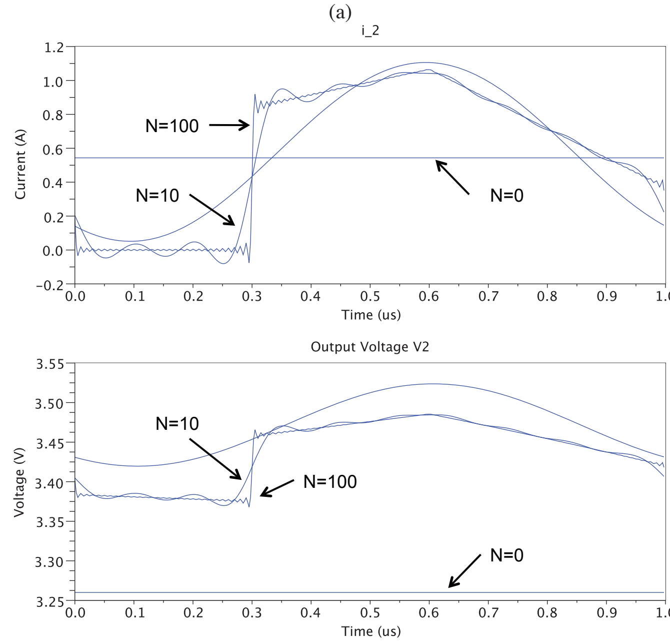

(b)

Fig. 4. Steady-state converter waveforms for different values of N. (a) $i_1(t)$ and $v_1(t)$. (b) $i_2(t)$ and $v_2(t)$.

The system parameters are as follows: f_s = 1 MHz, V_g = 5 V, L = 2 μH, r_L = 25 mΩ, C_1 = 20 μF, r_1 = 100 mΩ, C_2 = 2.2 μF, r_2 = 20 mΩ, R_1 = 10 Ω, R_2 = 6 Ω. The results from an accurate transient simulation using Spectre are shown as circles in Fig. 3(a), which confirms the accuracy of the frequency domain method. The output voltages and currents $i_1(t)$ and $i_2(t)$ are shown in Fig. 4 for N = {0,1,10,100} and D_B = 0.3. This illustrates how accurate voltage and current waveforms can be immediately obtained for a large range of operating conditions using the frequency domain technique, without resorting to lengthy time-domain simulations. The choice of N = 10 is a trade-off between accuracy and computational complexity. No substantial change in the average output voltage was found beyond N = 10.

This plot clearly shows the limitation of using $V_1\{0\}$ to obtain an accurate operating point. Note that the error converges to 0 for $D_A = D_B$. The discrepancy between the two sets of curves is dependent on the relative amplitude the ripple voltages and currents, since $V_1\{0\}$ converges to $V_1\{10\}$ for $\Delta i_L << i_L$. The load resistors R_1 and R_2 are selected such that $\Delta i_L / i_L < 1.2$ for the entire range of D_B. Under light-load conditions, as Δi_L approaches i_L, the error between

$V_1\{0\}$ and $V_1\{10\}$ can easily be above 25%. Assuming that the output voltages will have near zero steady-state error when the converter is operated in closed-loop, the exact duty cycles D_A and D_B are determined numerically to achieve the desired voltage operating point $V_1\{0\}$=$V_1\{10\}$ = 1.8 V and $V_2\{0\}$=$V_2\{10\}$ = 3.3 V, as shown in Fig. 3(b). Under these conditions, the standard method of (2) predicts steady-state duty ratios of D_A = 0.587 and D_B = 0.245, while using N = 10 gives D_A = 0.573 and D_B = 0.31. The resulting systematic error of ΔD_B = 6.5 % impacts the AC model for this operating point, as discussed in the following section.

III. Effect on Linearization

The linearization of the SIDO converter is given in [6] and repeated here for convenience. The small-signal output voltages $\hat{v}_1$ and $\hat{v}_2$ can be reconstructed from

$$\hat{v}_1 = G_{1A}\hat{d}_A + G_{1B}\hat{d}_B \tag{13}$$

and

$$\hat{v}_2 = G_{2A}\hat{d}_A + G_{2B}\hat{d}_B, \tag{14}$$

where the transfer functions for the two-input, two-output system are given by

[6]

$$G_{1A}(s) = \frac{\hat{v}_1(s)}{\hat{d}_A(s)} = \frac{V_g D_B Z_1(s)}{\delta(s)}$$

$$G_{1B}(s) = \frac{\hat{v}_2(s)}{\hat{d}_A(s)} = \frac{I_L Z_1(s)(D_B^{'} Z_2(s) + sL + r_L) + D_B Z_1(s)(V_2 - V_1)}{\delta(s)}$$

$$G_{2A}(s) = \frac{\hat{v}_1(s)}{\hat{d}_B(s)} = \frac{V_g(1 - D_B)Z_2(s)}{\delta(s)}$$

$$G_{2B}(s) = \frac{\hat{v}_2(s)}{\hat{d}_B(s)} = \frac{-I_L Z_2(s)(D_B Z_1(s) + sL + r_L) + D_B^{'} Z_2(s)(V_1 - V_2)}{\delta(s)}$$

where $\delta(s)$ is given by

$$\delta(s) = D_B^2 Z_1(s) + (1 - D_B)^2 Z_2(s) + sL + r_L \tag{15}$$

If the average output voltage is assumed to be constant, then the effect of using $V_1\{10\}$ instead of $V_1\{0\}$ is simply a shift in D_A and D_B, as highlighted in Fig. 3(b) and which causes a change in $\delta(s)$ through the factors $D_B^2 Z_1(s)$ and $(1-D_B)^2 Z_2(s)$. The effect of this error in D_B on $\delta(s)$ is more pronounced when Z_1 and Z_2 are significantly different, which occurs when the load currents are not equal. The transfer functions for the two operating points of Fig. 3(b) are shown in Fig. 5. The largest difference can be seen in G_{2B} and Z_{o22}.

IV. Conclusion

SIDO converters have been widely studied due to their cost advantages in applications that require multiple supply voltages. The steady-state operating points obtained from the standard averaging techniques, using the small ripple approximation were shown to differ significantly from the transient simulation results. Using the fourier based steady-state method with N = 10 produces a very close match with the transient simulations and is there recommended for future designs. The analysis presented in this work incorporates various parasitics and can easily be extended to MIMO converters having more then two outputs. The steady-state operating point unfortunately cannot be readily solved in closed-form for N = 0, however numerical techniques provide results for a wide range of operating conditions without having to resort to lengthy time-domain simulations.

Acknowledgment

The authors would like to thank NSERC for their support.

References

[1] R. Erickson and D. Maksimović, *Fundamentals of Power Electronics*. Kluwer Academic Publishers, 2001.

[2] D. Ma, W.-H. Ki, C.-Y. Tsui, and P. Mok, "A 1.8 v single-inductor dual-output switching converter for power reduction techniques," in *Symposium on VLSI Cicruits*, 2001, pp. 137–14.

[3] D. Trevisan, W. Stefanutti, P. Mattavelli, and P. Tenti, "FPGA control of simo dc-dc converters using load current estimation," in *Industrial Electronics Society, 2005. IECON 2005. 31st Annual Conference of IEEE*, nov. 2005.

[4] P. Patra, S. Samanta, A. Patra, and S. Chattopadhyay, "A novel control technique for single-inductor multiple-output dc-dc buck converters," in *Industrial Technology, 2006. ICIT 2006. IEEE International Conference on*, 15-17 2006, pp. 807 –811.

[5] A. Sharma and Y. Pavan, "A single inductor multiple output converter with adaptive delta current mode control," in *Circuits and Systems, 2006. ISCAS 2006. Proceedings. 2006 IEEE International Symposium on*, 0-0 2006, p. 4 pp.

[6] K.-Y. Lin, C.-S. Huang, D. Chen, and K. Liu, "Modeling and design of feedback loops for a voltage-mode single-inductor dual-output buck converter," in *Proc. IEEE Power Electronics Specialists Conference*, june 2008, pp. 3389 –3395.

[7] F. Misoc, M. Morcos, and J. Lookadoo, "Fourier-series models of dc-dc converters," in *Power Symposium, 2006. NAPS 2006. 38th North American*, 17-19 2006, pp. 193 –199.

[8] S. Sanders, J. Noworolski, X. Liu, and G. Verghese, "Generalized averaging method for power conversion circuits," *Power Electronics, IEEE Transactions on*, vol. 6, no. 2, pp. 251 –259, apr 1991.

[9] V. Caliskan, O. Verghese, and A. Stankovic, "Multifrequency averaging of dc/dc converters," *Power Electronics, IEEE Transactions on*, vol. 14, no. 1, pp. 124 –133, jan 1999.

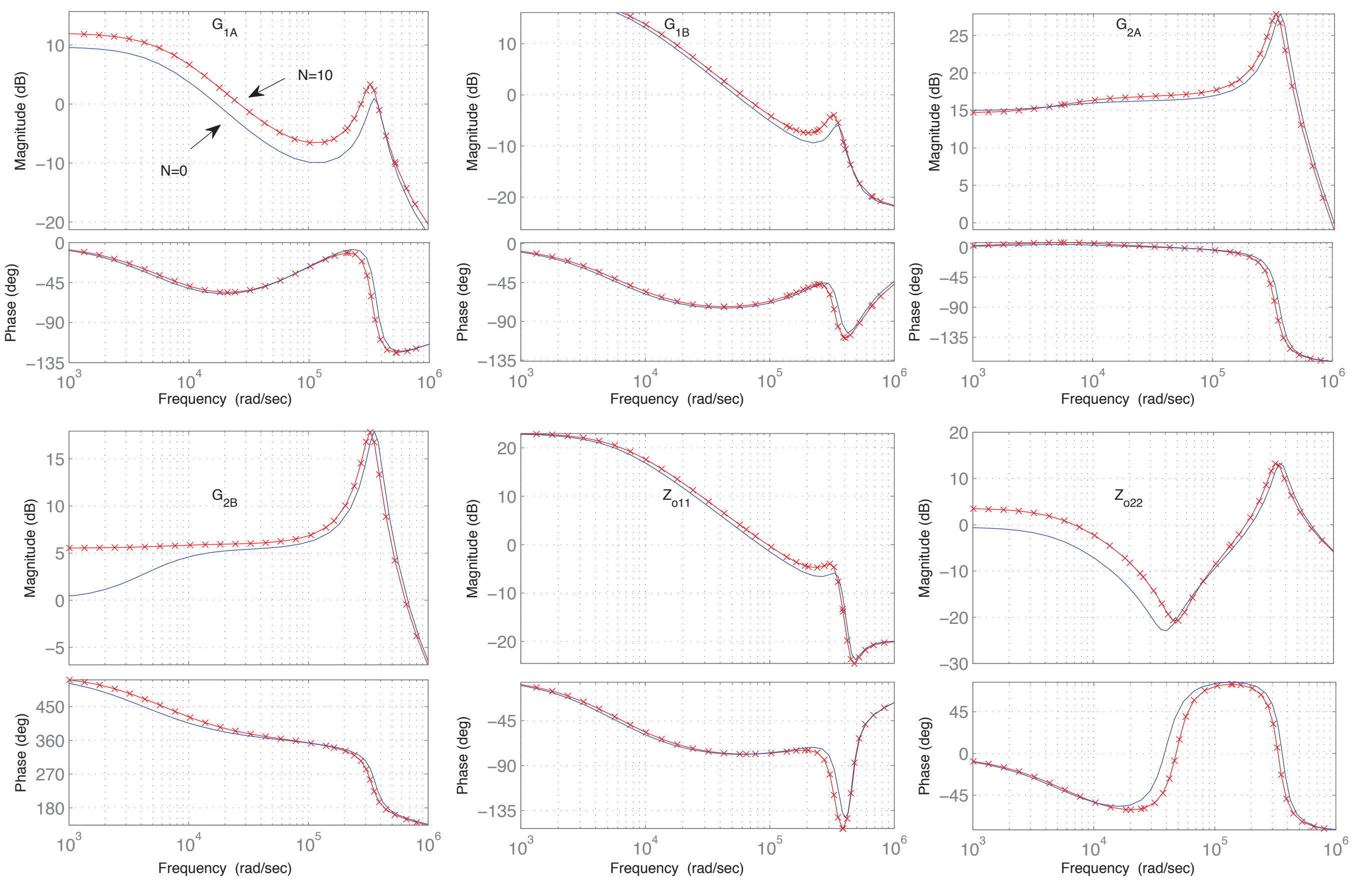

Fig. 5. Transfer functions for the SIDO converter corresponding to the two operating points in Fig. 3(b), corresponding to N=1 and N=10.